



Cite this: *Chem. Commun.*, 2016,
52, 8467

Received 15th April 2016,
Accepted 2nd June 2016

DOI: 10.1039/c6cc03185d

www.rsc.org/chemcomm

Solvent responsive catalyst improves NMR sensitivity *via* efficient magnetisation transfer†

Amy J. Ruddlesden and Simon B. Duckett*

A bidentate iridium carbene complex, $\text{Ir}(\kappa\text{C},\text{O}-\text{L}_1)(\text{COD})$, has been synthesised which contains a strongly electron donating carbene ligand that is functionalised by a *cis*-spanning phenolate group. This complex acts as a precursor to effective magnetisation transfer catalysts which form after reaction with H_2 and a suitable two electron donor. In solvents such as benzene, containing pyridine, they are exemplified by neutral, chiral $\text{Ir}(\text{H})_2(\kappa\text{C},\text{O}-\text{L}_1)(\text{py})_2$ with inequivalent hydride ligands and Ir–O bond retention, whilst in methanol, Ir–O bond cleavage leads to zwitterionic $[\text{Ir}(\text{H})_2(\kappa\text{C},\text{O}^- - \text{L}_1)(\text{py})_3]^+$, with chemically equivalent hydride ligands. The active catalyst's form is therefore solvent dependent. Both these complexes break the magnetic symmetry of the hydride ligands and are active in the catalytic transfer of polarisation from *parahydrogen* to a loosely bound ligand. Test results on pyridine, nicotinaldehyde and nicotine reveal up to $\approx 1.2\%$ single spin proton polarisation levels in their ^1H NMR signals which compare to the normal 0.003% level at 9.4 Tesla. These results exemplify how rational catalyst design yields a solvent dependent catalyst with good SABRE activity.

The use of hyperpolarisation methods to overcome the inherent insensitivity of NMR spectroscopy reflects an area of research where *Parahydrogen Induced Polarisation* (PHIP) features heavily.¹ The incorporation of *parahydrogen* ($p\text{-H}_2$), a nuclear singlet, into a molecule was first shown to produce an enhanced NMR signal in 1987.² The increase in signal intensity for resonances arising from, or coupled to, $p\text{-H}_2$ derived protons, has since been the subject of intense investigation. Recently a $p\text{-H}_2$ technique that does not chemically change a molecule, called Signal Amplification By Reversible Exchange (SABRE), has been developed.³ Polarisation is transferred through *J*-coupling between the $p\text{-H}_2$ derived hydride

ligands and the substrate ligands.³ Exchange with free substrate and fresh $p\text{-H}_2$ enables the build-up of polarisation in the substrate pool through multiple visits to the catalyst. The most commonly used catalysts are cationic species which contain either phosphine^{4,5} or N-heterocyclic carbene (NHC) ligands.^{6,7}

In fact, one of the most effective magnetisation transfer catalysts is $\text{Ir}(\text{COD})(\text{IMes})\text{Cl}^7$ [where IMes = 1,3-bis(2,4,6-trimethylphenyl)imidazole-2-ylidene, COD = cyclooctadiene] which forms the charged complex, $[\text{Ir}(\text{H})_2(\text{IMes})(\text{substrate})_3]\text{Cl}$ once activated with H_2 and a substrate. This SABRE catalyst contains chemically equivalent but magnetically inequivalent hydride ligands and polarisation transfer has proven particularly efficient in polar protic solvents such as methanol. Furthermore, using this catalyst a wide range of substrates including nicotinamide,^{8–10} isoniazid¹¹ and pyrazole¹² have been shown to become hyperpolarised. This type of approach has been exemplified for ^1H , ^{13}C , ^{31}P , ^{19}F and ^{15}N nuclei.^{5,13–15} However, due to the charged nature of such a species, it has proven less efficient in the range of low polarity solvents commonly used in NMR analysis.

It has also been shown that species with chemically inequivalent hydride ligands can act as SABRE catalysts. One reported example of this class of catalyst is given by $[\text{Ir}(\text{H})_2(\text{CH}_3\text{CN})(\text{IMes})(\text{PCy}_3)(\text{pyridine})]\text{Cl}$.¹⁶ Recently, a system that exhibits a wider solvent tolerance has been developed. It contains a bidentate ligand which binds through carbene and phenolate centres, resulting in a neutral catalyst in all solvents tested. While it was found to exhibit greater activity in non-polar solvents such as benzene,¹⁷ it was not efficient in methanol due to much slower ligand exchange.

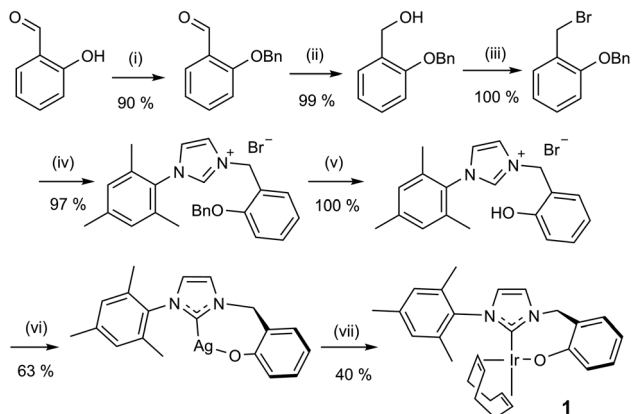
In this study, the related neutral iridium complex, $\text{Ir}(\kappa\text{C},\text{O}-\text{L}_1)(\text{COD})$, **1**, [where $\text{L}_1 = 3\text{-(2-methylene-phenolate)-1-(2,4,6-trimethylphenyl)imidazolylidene}$], has been synthesised starting from salicylaldehyde. It contains a *cis*-spanning phenolate-substituted bidentate NHC (see Scheme 1). Benzyl protection of the phenol¹⁸ allowed conversion of the aldehyde to the bromide¹⁹ *via* the alcohol.²⁰ Addition of 1-(2,4,6-trimethylphenyl)-1*H*-imidazole then formed the imidazolium bromide salt.²¹ Deprotection followed by silver carbene formation and subsequent transmetalation²²

Centre for Hyperpolarisation in Magnetic Resonance (CHyM), York Science Park,
University of York, Heslington, York, YO10 5NY, UK.

E-mail: simon.duckett@york.ac.uk; Tel: +44 (0)1904 322564

† Electronic supplementary information (ESI) available: Experimental details; synthesis and characterisation of compounds, SABRE experiments, kinetic data, activation parameters, UV-vis data. The underlying research data for this paper is available in accordance with EPSRC open data policy from DOI: 10.15124/cdaf969f-ba47-401e-876b-512c0eccc55c. See DOI: 10.1039/c6cc03185d



**Reagents and conditions:**

(i) Acetone, K_2CO_3 , BnBr, reflux, 2 h; (ii) $NaBH_4$, MeOH, 0 °C then r.t., 30 min; (iii) PBr_3 , DCM, r.t., 2 h; (iv) 1-(2,4,6-trimethylphenyl)-1H-imidazole, toluene, reflux, 18 h; (v) MeOH, $Pd(OH)_2/C$, H_2 , r.t., 20 h then 60 °C, 6 h; (vi) Ag_2O , DCM, r.t., 16 h; (vii) $[Ir(COD)Cl]_2$, THF, DCM, r.t., 4 h

Scheme 1 Synthetic route to **1**.

afforded the product, the phenoxide iridium carbene complex, **1**. Key compounds have been characterised by NMR and MS as illustrated in the ESI†

In solution, complex **1** appears yellow/orange in colour. UV-Vis analysis in DCM showed it exhibits three absorption bands in the visible region of the spectrum (373, 425 and 490 nm) with absorption coefficients in the range of charge transfer transitions (1017, 1326 and $249 \text{ dm}^3 \text{ mol}^{-1} \text{ cm}^{-1}$). Work by Perutz *et al.*^{23–26} has assigned similar bands in related square planar metal complexes to metal d–p transitions although earlier assignments suggested they were metal-to-ligand charge transfer bands.^{27–29}

At room temperature, the 1H NMR spectrum of complex **1** in CD_2Cl_2 yields well resolved resonances (see Fig. 1). Two doublets at δ 6.53 and 5.17 are observed for the CH_2 linker protons which have a common $^2J(HH)$ coupling of 14.9 Hz. These two protons are diastereotopic due to the seven-membered metallocycle which is indicative of the retention of the Ir–O bond.³⁰ Complex **1** is air/moisture sensitive but stable as a solid and in solution

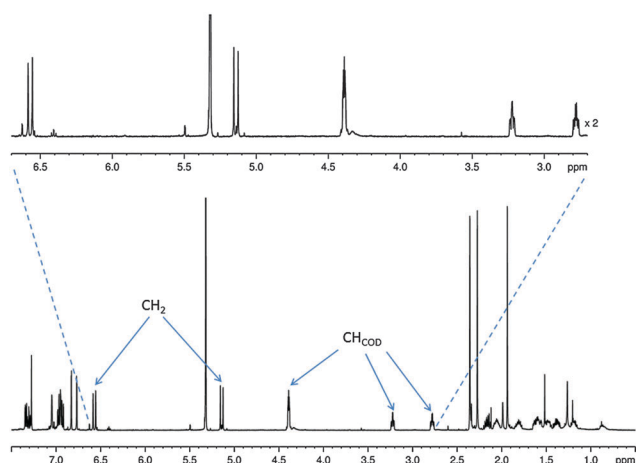


Fig. 1 1H NMR spectrum of **1** showing evidence for the diastereotopic CH_2 linker protons with key CH resonances labelled.

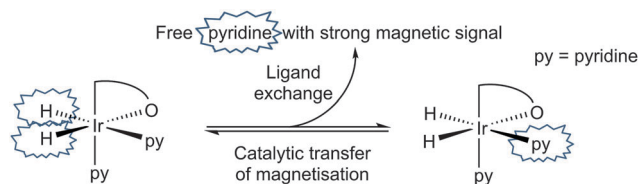
under N_2 . It also forms stable complexes once fully reacted with substrate and hydrogen as detailed in the following reactions.

Upon cooling a CD_2Cl_2 solution of complex **1** to 243 K all of its NMR signals become broad and undefined due to fluxional behaviour and when pyridine is added to this solution no reaction is evident. If, however, H_2 gas is added at 255 K, a limited reaction occurs as two pairs of hydride signals are now seen at δ –12.35 and –18.25 (1.7% conversion) and at δ –12.39 and –17.64 (0.6%). These minor hydride containing products are conformational isomers of compound **2** (see Scheme 3) which arise due to differing metallocycle orientations;³⁰ analogous behaviour has been reported.¹⁷

When *p*- H_2 is used in this reaction, these hydride ligand signals do not show any significant 1H NMR signal enhancement. However, the free H_2 signal in these spectra is substantial which suggests that **1** undergoes rapid and reversible oxidative addition of H_2 to form **2** which consumes the *p*- H_2 . There is no indication of the hydrogenation of COD at 255 K and upon warming to 298 K, these hydride signals broaden into the baseline of the corresponding NMR spectra and strong signals for **1** are always visible.

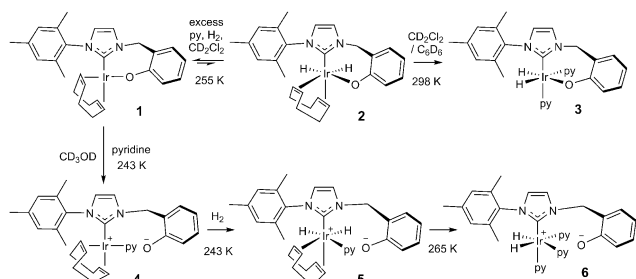
When a CD_2Cl_2 solution of **1** reacts with both pyridine and H_2 at 298 K a new neutral iridium species, $Ir(H)_2(\kappa C, O-L_1)(py)_2$, **3** is observed to slowly form containing two bound pyridine environments in a ratio of 1:1 (see ESI† for details). This species is also formed in C_6D_6 . The mutually coupled inequivalent hydride signals appear in CD_2Cl_2 at δ –22.55 and –25.49 ($^2J(HH) = 8.1 \text{ Hz}$) and in C_6D_6 at δ –21.94 and –24.52 ($^2J(HH) = 7.7 \text{ Hz}$). Their inequivalence suggests Ir–O bond retention, a fact which is further supported by the diastereotopic nature of the CH_2 linker protons which appear as doublets in both CD_2Cl_2 and C_6D_6 . Both complexes undergo pyridine and H_2 exchange as highlighted in Scheme 2, although only the pyridine ligand *trans* to hydride dissociates. The use of EXSY NMR³¹ experiments enabled determination of experimental rate constants for pyridine loss in **3** at 294 K of $3.74 \pm 0.06 \text{ s}^{-1}$ in CD_2Cl_2 and $13.5 \pm 0.6 \text{ s}^{-1}$ in C_6D_6 . The corresponding H_2 loss rates were $0.80 \pm 0.01 \text{ s}^{-1}$ and $3.02 \pm 0.07 \text{ s}^{-1}$ respectively and are therefore much slower than those of pyridine loss.

This behaviour changes significantly upon moving to protic methanol. Now, the addition of H_2 to a CD_3OD solution of complex **1** at 250 K, results in a very limited reaction to form a dihydride (<1%, with resonances at δ –12.65 and –18.27 and the low concentration presumably prevents observation of its conformational isomer) but upon warming further, rapid and total decomposition of **1** follows. In contrast, the addition of pyridine to a CD_3OD solution of complex **1** at 243 K forms the



Scheme 2 Transfer of hydride polarisation into the indicated pyridine ligand is followed by ligand exchange to build-up hyperpolarised pyridine in solution.





Scheme 3 Species formed during the reaction of **1** with H₂ and pyridine in CD₃OD (**4**, **5** and **6**) and CD₂Cl₂ (**2** and **3**) or C₆D₆ (**3**) solution.

phenolate dissociation product, square planar **4** quantitatively (see Scheme 3 and ESI[†]) where the COD ligand yields four inequivalent alkene proton resonances.

Upon the addition of *p*-H₂ and pyridine to **4** at 243 K, two PHIP enhanced hydride signals become immediately visible at δ -12.34 and -17.50 that are shown to couple *via* COSY. They arise from H₂ addition to **4** which initially forms the alkene dihydride complex, **5**. The CH₂ linker protons of **5** remain diastereotopic on phenolate rotation due to the absence of a mirror plane. Upon warming to 265 K, this system evolves further and a single hydride signal becomes visible at δ -22.18 due to the formation of [Ir(H)₂(κ C,O⁻L₁)(py)₃]⁺, **6**; the COD is converted to cyclooctene. Further NMR analysis confirms that **6** contains two bound pyridine ligand environments, in a 2:1 ratio, two hydride ligands and an iridium-carbene bond. Its CH₂ linker protons are now equivalent, appearing as a singlet at δ 4.83 due to the existence of a mirror plane as detailed in Scheme 3.

Complex **6** is zwitterionic, and its cationic Ir(III) centre is balanced by phenoxide ion formation. Hence the final reaction product formed from **1** with pyridine and H₂ is solvent dependent. The two pyridine ligands of **6** that lie *trans* to hydride are shown to dissociate with an experimental rate constant of 1.35 ± 0.03 s⁻¹ at 294 K, although no exchange of the pyridine *trans* to the carbene is observed. In CD₃OD, rapid H/D exchange, accompanied by HD formation, is observed which prevents the quantification of the H₂ loss rate in this solvent. At 294 K, the ligand exchange rates of species **3** in C₆D₆ are therefore much faster than those in CD₂Cl₂, but both are faster than those of **6** in CD₃OD as shown in the ESI.[†]

The ligand exchange rates of **6** in CD₃OH were examined as a function of temperature and activation parameters for these processes were calculated (see ESI[†]). The activation enthalpy values for both pyridine and hydride loss are very similar to each other (90.7 ± 1.6 kJ mol⁻¹ and 88.3 ± 9.1 kJ mol⁻¹ respectively). The entropy of activation values of 71.3 ± 5.3 J K⁻¹ and 56.1 ± 30.6 J K⁻¹ for pyridine and hydride loss respectively are also similar and positive thereby confirming the dissociative character of these steps.⁷ Similar ligand exchange processes, in a series of related complexes, yield values of similar size.^{7,32} A ligand exchange mechanism featuring reversible pyridine dissociation with H₂ loss *via* [Ir(κ C,O⁻L₁)(H)₂(H₂)(py)₂]⁺ is therefore indicated.³³

Both catalysts **3** and **6** therefore exhibit the substrate and H₂ exchange characteristics required for them to act as SABRE

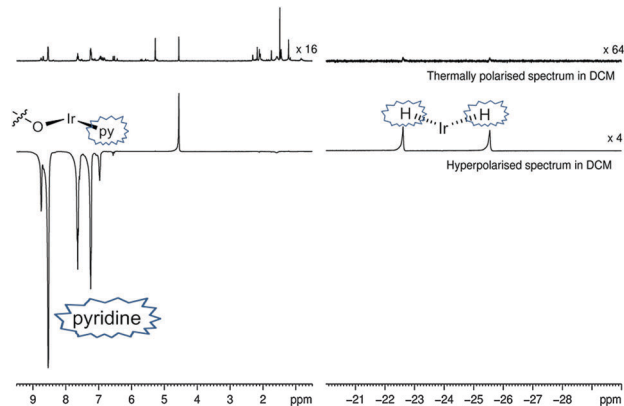


Fig. 2 Thermally polarised and hyperpolarised ¹H NMR spectra of a CD₂Cl₂ solution containing 0.06 M pyridine, 11 mol% **1** and 3 bars *p*-H₂. The enhanced signals for free and bound pyridine (in **3**) and the corresponding hydride ligands are indicated.

catalysts. To test their substrate signal enhancing performance, samples were prepared containing catalyst **1** and a chosen substrate in the desired NMR solvent. These were rigorously degassed before the addition of 3 bars of H₂. Samples were tested by reintroducing *p*-H₂ into the headspace of the NMR tube, shaking the sample in the low field outside of the spectrometer and then rapidly transferring the sample into the spectrometer for examination. This resulted in the observation of enhanced signals in the corresponding single scan ¹H NMR spectra for the hydride ligands, bound substrate and free substrate in solution as exemplified by Fig. 2. The total enhancement value seen for the five protons of pyridine in C₆D₆ proved to be 1850-fold under the conditions detailed. For CD₂Cl₂ this enhancement level was reduced to *ca.* 1660-fold whilst for CD₃OD solution it became 710-fold. Given the corresponding gain in signal-to-noise levels that these enhancements

Table 1 Maximum ¹H NMR SABRE enhancements (fold) observed for solutions containing pyridine (0.06 M and 11 mol% **1**), nicotinaldehyde (0.05 M and 14 mol% **1**) and nicotinic (0.04 M and 16 mol% **1**) in CD₂Cl₂, C₆D₆ and CD₃OD under 3 bars *p*-H₂

Solvent	Pyridine ¹ H NMR SABRE enhancement (fold)		
	<i>ortho</i>	<i>meta</i>	<i>para</i>
C ₆ D ₆	843 ± 27	600 ± 30	404 ± 13
CD ₂ Cl ₂	877 ± 32	337 ± 57	450 ± 22
CD ₃ OD	426 ± 5	47 ± 28	243 ± 3

Solvent	Nicotinaldehyde ¹ H NMR SABRE enhancement (fold)			
	H _A	H _B	H _C	H _D
C ₆ D ₆	259 ± 17	209 ± 22	118 ± 22	244 ± 18
CD ₂ Cl ₂	486 ± 36	400 ± 32	148 ± 34	396 ± 65
CD ₃ OD	62 ± 7	59 ± 10	26 ± 7	65 ± 6

Solvent	Nicotinic ¹ H NMR SABRE enhancement (fold)			
	H _A	H _B	H _C	H _D
C ₆ D ₆	400 ± 54	315 ± 48	88 ± 30	338 ± 80
CD ₂ Cl ₂	419 ± 51	381 ± 48	146 ± 44	386 ± 55
CD ₃ OD	29 ± 4	28 ± 3	3 ± 3	31 ± 3



provide, the resulting time savings are substantial in all solvents. For comparison purposes, the site specific enhancement values for the substrates pyridine, nicotinaldehyde and nicotine are summarised in Table 1. The performance of **1** as a SABRE catalyst for pyridine like substrates has therefore been established.

It is known that the amount of signal enhancement observed in the ^1H NMR spectrum of a substrate under SABRE is significantly affected by the ligand exchange rates, as previously explained by Green *et al.*³⁴ For comparison, $[\text{Ir}(\text{H})_2(\text{IMes})(\text{py})_3]\text{Cl}$, is commonly used as the catalyst benchmark for SABRE and its pyridine dissociation rate³² was found to be 23 s^{-1} . While the ligand dissociation rates for **3** and **6** are much lower, they still achieve good hyperpolarisation levels. In fact, these data show that one pyridine substrate *trans* to hydride in CD_2Cl_2 or C_6D_6 is more efficient at receiving SABRE than the two equivalent pyridine ligands of **6** in CD_3OD . Furthermore, the concept of an active solvent responsive catalyst is illustrated.

In summary, the iridium precatalyst $\text{Ir}(\kappa\text{C},\text{O}-\text{L}_1)(\text{COD})$, **1** containing a phenolate substituted NHC has been synthesised and shown to act as an efficient SABRE catalyst precursor. The active catalytic species is solvent dependent. Complex **1** contains an Ir–O bond which is affected by solvent polarity and proton availability; in non-polar C_6D_6 and polar aprotic CD_2Cl_2 , this bond is strong and substitution resistant with **1** forming $\text{Ir}(\kappa\text{C},\text{O}-\text{L}_1)(\text{H})_2(\text{py})_2$ (**3**) on reaction with H_2 and pyridine. In contrast, on changing to polar protic methanol, the Ir–O bond becomes labile and the phenolate easily dissociates from the iridium centre, such that zwitterionic $[\text{Ir}(\kappa\text{C},\text{O}^--\text{L}_1)(\text{H})_2(\text{py})_3]^+$ (**6**) forms. **6** is directly analogous to the efficient SABRE catalyst $[\text{Ir}(\text{H})_2(\text{IMes})(\text{py})_3]\text{Cl}$ which performs well in CD_3OD but has lower activity in non-polar CD_2Cl_2 and C_6D_6 . Both **3** and **6** undergo pyridine and H_2 exchange thereby enabling them to act as SABRE catalysts. Whilst **6** works well in CD_3OD , catalyst neutrality in the non-polar solvents CD_2Cl_2 and C_6D_6 results in the formation of **3** which is highly active for SABRE catalysis. This study therefore shows that catalyst design and control can lead to improved magnetisation transfer in a range of solvents, a requirement for future studies that seek to identify low concentration analytes^{35–37} and to produce hyperpolarised MRI contrast agents.

We acknowledge Bruker Biospin and the EPSRC for a studentship (1359398) and the Wellcome Trust and Wolfson Foundation (092506 and 098335) for their generous funding. We thank Dr Jason Lynam, Prof. Gary Green and Dr Ryan Mewis for helpful comments.

References

- 1 T. C. Eisenschmid, R. U. Kirss, P. P. Deutsch, S. I. Hommeltoft, R. Eisenberg, J. Bargon, R. G. Lawler and A. L. Balch, *J. Am. Chem. Soc.*, 1987, **109**, 8089.
- 2 C. R. Bowers and D. P. Weitekamp, *J. Am. Chem. Soc.*, 1987, **109**, 5541.
- 3 R. W. Adams, S. B. Duckett, R. A. Green, D. C. Williamson and G. G. R. Green, *J. Chem. Phys.*, 2009, **131**, 194505.
- 4 K. D. Atkinson, M. J. Cowley, S. B. Duckett, P. I. P. Elliott, G. G. R. Green, J. Lopez-Serrano, I. G. Khazal and A. C. Whitwood, *Inorg. Chem.*, 2009, **48**, 663.
- 5 K. D. Atkinson, M. J. Cowley, P. I. P. Elliott, S. B. Duckett, G. G. R. Green, J. Lopez-Serrano and A. C. Whitwood, *J. Am. Chem. Soc.*, 2009, **131**, 13362.
- 6 B. J. A. van Weerdenburg, S. Glogglar, N. Eshuis, A. H. J. Engwerda, J. M. M. Smits, R. de Gelder, S. Appelt, S. S. Wymenga, M. Tessari, M. C. Feiters, B. Blumich and F. P. J. T. Rutjes, *Chem. Commun.*, 2013, **49**, 7388.
- 7 M. J. Cowley, R. W. Adams, K. D. Atkinson, M. C. R. Cockett, S. B. Duckett, G. G. R. Green, J. A. B. Lohman, R. Kerssebaum, D. Kilgour and R. E. Mewis, *J. Am. Chem. Soc.*, 2011, **133**, 6134.
- 8 J.-B. Hoeverner, N. Schwaderlapp, R. Borowiak, T. Lickert, S. B. Duckett, R. E. Mewis, R. W. Adams, M. J. Burns, L. A. R. Highton, G. G. R. Green, A. Olaru, J. Hennig and D. von Elverfeldt, *Anal. Chem.*, 2014, **86**, 1767.
- 9 R. E. Mewis, K. D. Atkinson, M. J. Cowley, S. B. Duckett, G. G. R. Green, R. A. Green, L. A. R. Highton, D. Kilgour, L. S. Lloyd, J. A. B. Lohman and D. C. Williamson, *Magn. Reson. Chem.*, 2014, **52**, 358.
- 10 M. L. Truong, F. Shi, P. He, B. Yuan, K. N. Plunkett, A. M. Coffey, R. V. Shchepin, D. A. Barskiy, K. V. Kovtunov, I. V. Koptyug, K. W. Waddell, B. M. Goodson and E. Y. Chekmenev, *J. Phys. Chem. B*, 2014, **118**, 13882.
- 11 H. Zeng, J. Xu, J. Gillen, M. T. McMahon, D. Artemov, J.-M. Tyburn, J. A. B. Lohman, R. E. Mewis, K. D. Atkinson, G. G. R. Green, S. B. Duckett and P. C. M. van Zijl, *J. Magn. Reson.*, 2013, **237**, 73.
- 12 E. B. Dücker, L. T. Kuhn, K. Münnemann and C. Griesinger, *J. Magn. Reson.*, 2012, **214**, 159.
- 13 A. N. Pravdivtsev, A. V. Yurkovskaya, H. Zimmermann, H.-M. Vieth and K. L. Ivanov, *RSC Adv.*, 2015, **5**, 63615.
- 14 L. T. Kuhn, U. Bommerich and J. Bargon, *J. Phys. Chem. A*, 2006, **110**, 3521.
- 15 V. V. Zhivonitko, I. V. Skovpin and I. V. Koptyug, *Chem. Commun.*, 2015, **51**, 2506.
- 16 M. Fekete, O. Bayfield, S. B. Duckett, S. Hart, R. E. Mewis, N. Pridmore, P. J. Rayner and A. Whitwood, *Inorg. Chem.*, 2013, **52**, 13453.
- 17 A. J. Ruddlesden, R. E. Mewis, G. G. R. Green, A. C. Whitwood and S. B. Duckett, *Organometallics*, 2015, **34**, 2997.
- 18 V. L. Schuster, Y. Chi, A. S. Wasmuth and R. S. Pottorf, G. L. Olson and W. I. P. Organisation, *WO2011/37610 A1*, Albert Einstein College Of Medicine Of Yeshiva University, US, 2011.
- 19 G. Sagrera and G. Seoane, *Synthesis*, 2009, 4190.
- 20 R. V. Somu, H. Boshoff, F. Qiao, E. M. Bennett, C. E. Barry and C. C. Aldrich, *J. Med. Chem.*, 2005, **49**, 31.
- 21 G. Occhipinti, V. R. Jensen, K. W. Tornroos, N. A. Froystein and H. R. Bjorsvik, *Tetrahedron*, 2009, **65**, 7186.
- 22 J. L. Herde, J. C. Lambert and C. V. Senoff and M. A. Cushing, *Inorg. Syn.*, John Wiley & Sons, Inc., 2007.
- 23 M. V. Campian, R. N. Perutz, B. Procacci, R. J. Thatcher, O. Torres and A. C. Whitwood, *J. Am. Chem. Soc.*, 2012, **134**, 3480.
- 24 M. C. Nicasio, R. N. Perutz and A. Tekkaya, *Organometallics*, 1998, **17**, 5557.
- 25 L. Cronin, M. C. Nicasio, R. N. Perutz, R. G. Peters, D. M. Roddick and M. K. Whittlesey, *J. Am. Chem. Soc.*, 1995, **117**, 10047.
- 26 C. Hall, W. D. Jones, R. J. Mawby, R. Osman, R. N. Perutz and M. K. Whittlesey, *J. Am. Chem. Soc.*, 1992, **114**, 7425.
- 27 G. L. Geoffroy, H. Isci, J. Litrenti and W. R. Mason, *Inorg. Chem.*, 1977, **16**, 1950.
- 28 R. Brady, B. R. Flynn, G. L. Geoffroy, H. B. Gray, J. Peone and L. Vaska, *Inorg. Chem.*, 1976, **15**, 1485.
- 29 G. L. Geoffroy, G. S. Hammond and H. B. Gray, *J. Am. Chem. Soc.*, 1975, **97**, 3933.
- 30 H. M. Peng, R. D. Webster and X. Li, *Organometallics*, 2008, **27**, 4484.
- 31 K. Stott, J. Keeler, Q. N. Van and A. J. Shaka, *J. Magn. Reson.*, 1997, **125**, 302.
- 32 L. S. Lloyd, A. Asghar, M. J. Burns, A. Charlton, S. Coombes, M. J. Cowley, G. J. Dear, S. B. Duckett, G. R. Genov, G. G. R. Green, L. A. R. Highton, A. J. J. Hooper, M. Khan, I. G. Khazal, R. J. Lewis, R. E. Mewis, A. D. Roberts and A. J. Ruddlesden, *Catal. Sci. Technol.*, 2014, **4**, 3544.
- 33 D. A. Barskiy, A. N. Pravdivtsev, K. L. Ivanov, K. V. Kovtunov and I. V. Koptyug, *Phys. Chem. Chem. Phys.*, 2016, **18**, 89.
- 34 R. A. Green, R. W. Adams, S. B. Duckett, R. E. Mewis, D. C. Williamson and G. G. R. Green, *Prog. Nucl. Magn. Reson. Spectrosc.*, 2012, **67**, 1.
- 35 N. Eshuis, N. Hermkens, B. J. A. van Weerdenburg, M. C. Feiters, F. P. J. T. Rutjes, S. S. Wymenga and M. Tessari, *J. Am. Chem. Soc.*, 2014, **136**, 2695.
- 36 N. Eshuis, R. L. E. G. Aspers, B. J. A. van Weerdenburg, M. C. Feiters, F. P. J. T. Rutjes, S. S. Wymenga and M. Tessari, *Angew. Chem., Int. Ed.*, 2015, **54**, 14527.
- 37 N. Eshuis, B. J. A. van Weerdenburg, M. C. Feiters, F. P. J. T. Rutjes, S. S. Wymenga and M. Tessari, *Angew. Chem., Int. Ed.*, 2015, **54**, 1481.

